

# A probabilistic uncertainty evaluation method for turbomachinery probe measurements

Thomas Behr<sup>1\*</sup>, Anestis I. Kalfas<sup>2†</sup>, and Reza S. Abhari<sup>1‡</sup>

<sup>1</sup>ETH, Turbomachinery Laboratory, Zurich, Switzerland

<sup>2</sup>AUTH, Department of Mechanical Engineering, Laboratory of Fluid Mechanics and Turbomachinery, Thessaloniki, Greece

**Abstract.** The paper presents a probabilistic uncertainty evaluation method described in the Guide to the Expression of Uncertainty in Measurement (GUM) [1] and its application to the field of Turbomachinery probe measurement techniques. All sources of uncertainties contributing to a measurement result are expressed in terms of probability distributions. Consequently, the overall standard uncertainty of the result can be calculated using the Gaussian error propagation formula. The result of the uncertainty evaluation yields the most probable value of the measurand and describes its distribution in terms of standard or extended uncertainties. A pneumatic five-hole-probe measurement technique has been chosen to show the principle of the probabilistic uncertainty evaluation method. The complete signal chain including the probe calibration, the modeling and the application in the turbine has been included in the analysis. The overall uncertainties of the measured flow angles and flow total and static pressures are presented as a function of the flow Mach number. In addition, the contribution of the individual sources of uncertainty to the overall standard uncertainty is shown. Based on this break down of uncertainties optimization options of the measurement chain are suggested.

## 1 Introduction

A realistic determination of the uncertainties of a measurement is essential for the further usage of the results. In the field of Turbomachinery the validation of numerical tools or the performance evaluation of components based on experimental results needs knowledge about their uncertainty.

The first and most important part on this way is the detection of all sources of uncertainty influencing the results. In most cases their related information appear in very different formats, i.e. data sheet information on accuracy of measurement systems, stochastic distributions, etc., which can not be directly combined. In some cases different sources of uncertainty correlate with each other and should not be added directly. Unlike previously used methods the Guide of Uncertainty in Measurements describes a standardized method, which first converts all uncertainty information in probability distributions. Based on this it is consistent to use only the Gaussian error propagation formula to derive the overall uncertainty. In case of correlated parameters, cross-correlation coefficients are used to evaluate their combined uncertainty contribution. Consequently, the final statement of uncertainty of the measurement result

contains the limits and the distribution of the expected values.

The systematic approach of this method gives as well an overview about the share of each source of uncertainty to the overall uncertainty. These information can be used in order to optimize measurement chains.

This paper will introduce this probabilistic uncertainty evaluation method by applying it to the field of flow field measurements in turbomachines with a pneumatic five-hole probe. The uncertainty analysis of the measurement chain is presented in a general way, such that it can be easily adapted to different types of probes or calibration coefficients. Different probe data evaluation algorithms will be analyzed and compared.

## Nomenclature

|             |   |     |
|-------------|---|-----|
| $K_\varphi$ | Calibration coefficient of flow yaw angle   | [-] |
| $K_\gamma$  | Calibration coefficient of flow pitch angle | [-] |
| $K_s$       | Calibration coefficient of static pressure  | [-] |
| $K_t$       | Calibration coefficient of total pressure   | [-] |

\* Thomas Behr: [thomas.behr@ch.abb.com](mailto:thomas.behr@ch.abb.com)

† Anestis I. Kalfas: [akalfas@auth.gr](mailto:akalfas@auth.gr)

‡ Reza S. Abhari: [abhari@lec.mavt.ethz.ch](mailto:abhari@lec.mavt.ethz.ch)

|   |                      |      |
|---|----------------------|------|
| p | Pressure             | [Pa] |
| u | Standard uncertainty |      |
| x | Input parameter      |      |
| y | Result parameter     |      |
| V | Variance             |      |
| k | Coverage factor      |      |

**Greek**

|           |                  |     |
|-----------|------------------|-----|
| $\varphi$ | Flow yaw angle   | [°] |
| $\gamma$  | Flow pitch angle | [°] |

**Abbreviations**

|     |   |
|-----|---|
| 5HP | 5-Hole-Probe  |
| GEP | Gaussian error propagation                                |
| GUM | Guide to the expression of uncertainty in measurement [1] |

**Subscripts**

|   |                   |
|---|-------------------|
| c | Calibration       |
| m | Measurement       |
| s | static            |
| t | total             |
| M | Model             |
| P | Pressure DAQ      |
| R | Reference Flow    |
| T | Traversing system |

**2 Uncertainty evaluation method**

Unlike the traditional approaches the GUM method does not assume that there is a ‘true’ value that has to be determined during a measurement. Rather the methods recognizes that in the measurement of a physical parameter its value is only determined at the time of the measurement. Since the knowledge about a measurement is always incomplete, this determined value is never unique. Out of this idea a definition of the measurement uncertainty arises:

*The measurement uncertainty is a value associated to the physical parameter, which characterizes the range of values that can be rationally assigned to the physical parameter from the knowledge about the measurement.*

Consequently, the goal of the uncertainty analysis has to be to make a statement about the physical parameters determined by a measurement process, which is not entirely known. On this path there are two main focus points to consider:

- measurement chain (model, physical relation)
- input values (probability distributions)

Based on this strategy the evaluation procedure can be structured in four logical steps proposed by Weise and Wöger [2]:

Step 1 - Development of a mathematical model based on the definition of the measurand that describes the measurement problem.

Step 2 - Gathering of uncertainty information (observations, data sheets, etc.) and converting them to probability distributions

Step 3 - Calculation of the result and the associated standard uncertainty by applying the model and propagating the uncertainties.

Step 4 - Presentation of the result and its extended uncertainty.

Within step 2 all information about the input data have to be expressed by probability distributions. Due to this it is correct to use the Gaussian uncertainty propagation method, which is appropriate to combine these kind of information.

The GUM method differentiates between two types of knowledge about the input data:

- Type A

Statistical information gathered during the measurement (observed data)

- Type B

Non-statistical information, which are known prior to the measurement (data sheets, etc.)

As an example of type B the uncertainty information of a measurement device can be considered, for which only the lower and upper limit are known. In this case a rectangular distribution can be used.

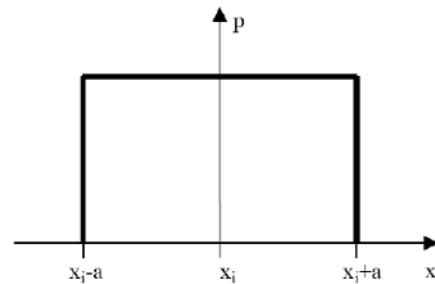


Fig. 1. Rectangular distribution

The variance will be calculated as

$$V(X) = \frac{(2a)^2}{12} \tag{2}$$

The standard uncertainty will be calculated as

$$u(x) = \sqrt{V(X)} = \frac{a}{\sqrt{3}} \tag{3}$$

The uncertainty contribution of each input parameter on the result can be calculate using its partial derivative

$$u_i(y) = \frac{\partial y}{\partial x_i} \cdot u(x_i) \tag{4}$$

Finally, the law of uncertainty propagation is used to calculate the standard uncertainty of the result, which represents a level of confidence of 67%.

$$u(y) = \sqrt{\sum_{i=1}^n u_i^2(y)} \tag{5}$$

The GUM method uses a term called ‘expanded’ uncertainty U(y). It is defined as

$$U(y) = k \cdot u(y) \tag{6}$$

It includes the coverage factor k. k=2 represents a level of confidence of 95% if the result is normal distributed. The coverage factor should be always stated, if the extended

uncertainty is presented to be able to recalculate the standard uncertainty. Due to its structured type the method can be well automated and implemented in software applications. This investigation has been supported by the software tool ‘GUM Workbench®’ [3].

### 3 Experimental method

#### 3.1 Cobra-head pneumatic five-hole probe

The method of the uncertainty evaluation will be demonstrated on a miniature cobra-head pneumatic five-hole probe (see Figure 2). This probe uses four tubes arranged around a center tube to measure the pressure in a flow path of a turbomachine. The tip of the probe is shaped as a pyramid such that all holes are facing a different direction. It has a diameter of 0.9 mm. The advantage of the cobra-head shape is that all holes on the circumference of the probe head show a similar pressure sensitivity to angle variations. A further advantage is the large distance (about 5 tip diameter) of the measurement volume from the probe body.

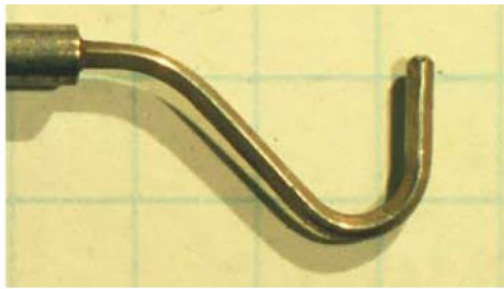


Fig. 2. Cobra-head pneumatic five-hole probe

Depending on the incoming flow, the holes of the probe will experience a certain pressure. Figure 3 shows the contours of the hole pressures for different yaw and pitch angles, non-dimensionalized with the flow total and static pressure according to equation (7). The center hole has a low pressure sensitivity to angle variations. In the center position it functions like a pitot probe, which can be seen by a  $C_p$  value of 1, which is identical to the flow total pressure.

$$Cp_i = \frac{p_i - p_s}{p_t - p_s} \text{ with } i = 1 \dots 5 \quad (7)$$

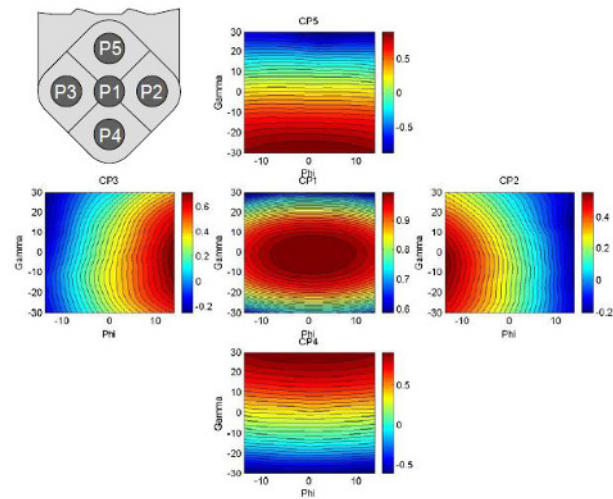


Fig. 3. Pressure coefficient contours of a five-hole probe at  $Ma=0,25$

#### 3.2 Freejet calibration facility

Aerodynamic probes can be calibrated in the freejet facility of the ETH Turbomachinery Laboratory up to Mach numbers of 0.9. Therefore a probe can be mounted in a traversing system, which allows a yaw angle variation of  $\pm 360^\circ$  ( $\Delta\varphi_{c,T} = \pm 0.01^\circ$ ). This probe support system is fixed to a table, which can be inclined between pitch angles of  $\pm 30^\circ$  ( $\Delta\gamma_{c,T} = \pm 0.015^\circ$ ). A computer system controls automatically the probe positioning, the data acquisition as well as the operation of the calibration rig. The axisymmetric freejet flow has a uniform velocity profile and a turbulence level of about 0.3%. The diameter of the nozzle exit is 100mm. A stochastic deviation between the aerodynamic and geometric flow angle has been determined to be  $\Delta\varphi_{c,R} = \Delta\varphi_{c,R} = \pm 0.015^\circ$ .

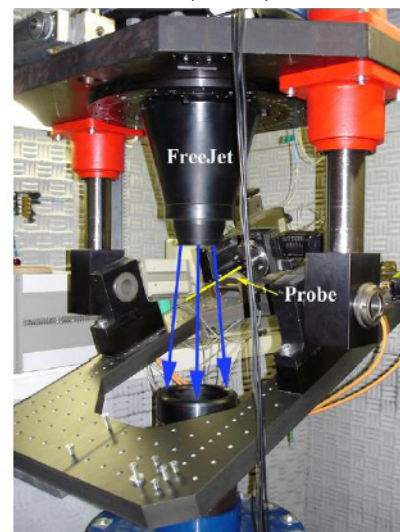


Fig. 4. Freejet probe calibration facility

### 3.3 Axial turbine test rig LISA

The turbine test rig considered for this investigation is the axial turbine facility ‘LISA’ of the ETH Turbomachinery Laboratory. Mach numbers within the turbine flow are in the range of 0.1 to 0.6. The height of the flow path is 70 mm. More details on the rig and the turbine flow fields can be found in Behr et al. [4]. Area traverses within the turbine can be performed by using an automated multi-axis probe traversing system with an positioning accuracy of  $\Delta\varphi_{m,T} = \Delta\gamma_{m,T} = \pm 0.015^\circ$ .

### 3.4 Probe pressure data acquisition system

A mobile unit containing 5 Keller differential pressure sensors (PR33X, 0.5bar) and 1 Keller absolute pressure sensor (PAA33X, 1bar) is used for measuring the probe pressures relative to atmosphere and the atmospheric pressure. The accuracy of these sensors is 0.05% FS. The same unit is used for calibration and measurement. Since the unit can be placed close to the probe, the total length of the pressure tubes from probe tip to sensor reduces to about 1m, which yields a short pressure settling time.

## 4 Uncertainty of flow yaw and pitch angle

### 4.1 Description of the measurement chain

To derive flow angle information of turbine flows, angle sensitive pressures probe are commonly used. Before a probe can be used it has to be calibrated within a reference flow. For this purpose the uniform freejet flow provides a flow field with well know parameters. The probe head is positioned in the center region of the flow where streamlines are supposed to be parallel. During the calibration the probe will be inclined according to a matrix of different yaw and pitch angles relative to the flow. For each position the pressures of all probe holes will be recorded. From these pressures the calibration coefficients for the yaw ( $K\varphi$ ) and the pitch axis ( $K\gamma$ ) can be calculated. In this way every adjusted yaw and pitch angle position of the probe can be assigned to a pair of  $K\varphi$  and  $K\gamma$ .

Later during the probe application within an unknown turbine flow the pressures at the probe tip will be recorded. From these the coefficients  $K\varphi$  and  $K\gamma$  can be calculated. These pair of coefficients can be related clearly to a pair of yaw and pitch angles by using the calibration information.

#### 4.1.1 Step 1 – Model of the measurement chain

The algorithm which has been explained in the previous section has been put into a flow chart diagram (see Figure 5). It is divided into two logical parts, which are the calibration of the probe and the measurement in an unknown flow. The yellow boxes represent values of uncertainty of parameters, whereas the blue boxes stand for mathematical conversions. In this way the propagation

of uncertainties into the final result can be visualized. The sources of uncertainty are especially indicated and will be discussed in the next section.

The calibration coefficients  $K\varphi$  and  $K\gamma$  are defined as follows:

$$K\varphi(\varphi, \gamma, Ma) = \frac{p_2 - p_3}{q} \quad (8)$$

and

$$K\gamma(\varphi, \gamma, Ma) = \frac{p_4 - p_5}{q} \quad (9)$$

To non-dimensionalize the coefficients and to relate the angle-sensitive pressure differences to the flow dynamic head, a denominator  $q$  is defined as:

$$q = p_1 - \frac{1}{4} \sum_{i=2}^5 p_i \quad (10)$$

Figure 6 shows the distribution of calibration coefficients  $K\varphi$  and  $K\gamma$  with respect to yaw and pitch angles at a constant Mach number of  $Ma=0.25$ . From the contour lines it can be clearly seen that each coefficient shows a nearly constant

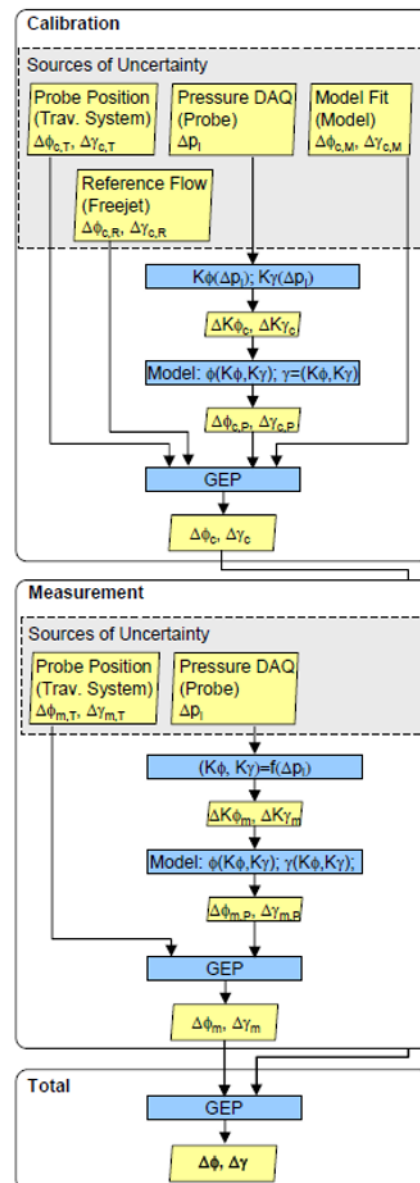
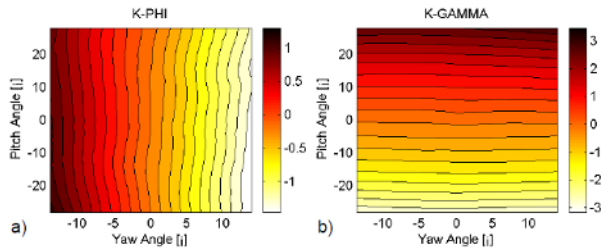


Fig. 5. Uncertainty propagation of flow angle measurement



**Fig. 6.** Distribution of calibration coefficients with respect to yaw and pitch angles at  $Ma = 0.25$ , a)  $K\phi$  b)  $K\gamma$   
 gradient in its direction of sensitivity and a zero gradient in the orthogonal direction. This fact confirms that both coefficients are well decoupled.

#### 4.1.2 Step 2 – Uncertainty information

##### Probe Position, Reference Flow

Angle uncertainties arising from the probe traversing systems and the deviation of the reference are given by the specification of the experimental facilities. Since no better information are available rectangular distributions are assumed for the parameter uncertainties.

##### Model Fit

After the calibration angles and calibration coefficients are related as

$$K\phi(\phi, \gamma) \text{ and } K\gamma(\phi, \gamma) \quad (11)$$

For the post processing of measurement data these relation has to be inverted to

$$\phi(K\phi, K\gamma) \text{ and } \gamma(K\phi, K\gamma) \quad (12)$$

in order to get direct expressions of  $\phi$  and  $\gamma$ . One possibility is to approximate the functions of (12) with two-dimensional polynomials in the form

$$\phi = \sum_{i=0}^m \sum_{j=0}^n a_{\phi,ij} \cdot K\phi^i \cdot K\gamma^j \quad (13)$$

$$\gamma = \sum_{i=0}^m \sum_{j=0}^n a_{\gamma,ij} \cdot K\phi^i \cdot K\gamma^j \quad (14)$$

A least square fit method can be applied to determine the polynomial coefficients. The degree of the polynomial will define how well it fits to the points of the calibration. Higher order polynomials are more likely to have a good fit on the points of the calibration, however they are also more likely to introduce unphysical oscillation in between the calibrated points. Lower order polynomials are more continuous, but will have difficulties to fit a wider range of calibrated flow angles. The quality of the polynomial fit can be determined by calculating the difference of the calibrated flow angles and the angles which are derived by the polynomial approximation.

An alternative to polynomials can be the use of look-up tables. In this case the parameters of (11) are rearranged according to (12). Any angle in between the calibrated points will be calculated by a two-dimensional interpolation, preferably of second or third order.

In order to decide which method is better the following consideration can be made. The best known description of the freejet reference flow is given at the calibrated angular

positions. The uncertainty at these points can be reduced further by using averages out of repeated pressure measurements. A polynomial approximation, which deviates also at the calibrated angular positions, will therefore increase the uncertainty. In case of look-up tables, these points can be reproduced exactly. For angular position in between the calibrated points, the two-dimensional interpolation of low order yields values, which are on a continuous surface in between the supporting points. For these reasons look-up tables should be favored.

##### Pressure DAQ

Another source of uncertainty comes from the pressure data acquisition system. The measurement of the probe pressures is associated with an uncertainty depending on factors such as accuracy, stability, sensitivity of the pressure sensor, resolution of the DAQ boards, etc. In the current case the specification of the manufacturer yielded the required information. Since no information on the distribution have been available a rectangular distribution has been assumed. The pressure uncertainties will propagate into the calibration coefficients  $K\phi$  and  $K\gamma$ . In order to determine their effect on the angles, the analytical descriptions of equations (13,14) of the relation between angles and calibration coefficients have been used. For this purpose an exact fit on the calibration data can be assumed.

Further sources of uncertainty are eliminated if for calibration and measurement the same pressure measurement system is used. The mobile pressure measurement unit of the current investigation has been designed to follow this idea.

#### 4.1.3 Step 3 – Uncertainty calculation

According to the flow chart of Figure 6 the uncertainties have been calculated for a selection of calibrated angular positions each at 4 different Mach numbers.

The fit of the polynomial model has been calculated at all calibrated points. The resulting difference could be summarized for each Mach number with a value of the standard deviation based on a normal distribution. The uncertainty of the model fit has been included in the calculation in this format.

The fit of the look-up table has been assumed to be ideal, with a zero uncertainty.

The uncertainty of the pressure measurement has been calculated for each of the selected sample points.

#### 4.1.4 Step 4 – Results

To evaluate the contribution of each source of uncertainty on the overall uncertainty the square of the propagated uncertainties  $u_i^2(y)$  can be compared. Figure 7 shows the shares of uncertainty of one example point at four different Mach numbers. It can be seen that the traversing systems as well as the angle deviations of the reference flow do not contribute significantly to the overall uncertainty. The model fit of the calibration polynomial gives at all Mach numbers a constant contribution.

Uncertainties of the pressure measurement system are dominant at low Mach numbers ( $Ma=0.16$ ) and negligible at higher Mach numbers ( $Ma=0.53$ ). It is therefore of high importance for an optimal angle uncertainty to select an appropriate sensor pressure range.

The contribution of calibration and measurement on the overall uncertainty is illustrated in Figure 8. In this case, at higher Mach numbers ( $Ma=0.53$ ) the polynomial fit contributes with over 95% to the angle uncertainty.

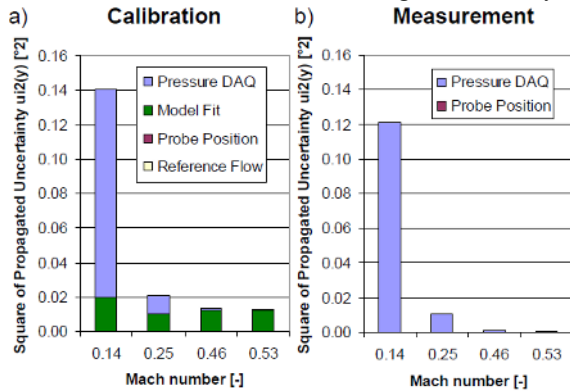


Fig. 7. Square of propagated uncertainties  $u_i^2(y)$  [  $^\circ^2$  ] of four Mach numbers [-] a) Calibration b) Measurement (using Calibration polynoms)

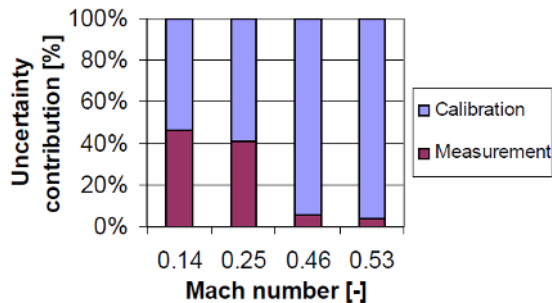


Fig. 8. Uncertainty contribution of calibration and measurement of four Mach numbers [-] (using Calibration polynoms)

The expanded uncertainties of flow yaw and pitch angle versus Mach number are illustrated in Figure 9. The uncertainties of 8 different sample points have been averaged to create these graphs. A coverage factor of  $k=2$  has been applied to derive the expanded uncertainty. Therefore the values shown have a level of confidence of 95% and are normal distributed. It can be seen that the uncertainty increases exponentially towards low Mach numbers if the pressure sensors are kept the same. With the experimental setup investigated the expanded uncertainty at low Mach numbers ( $Ma=0.14$ ) increases up to  $u(y)=\pm 1^\circ$ , whereas at high Mach numbers ( $Ma=0.53$ ) they are as low as  $u(y)=\pm 0.3^\circ$  if calibration polynoms are used. If the uncertainty of the polynoms can be replaced by the lower uncertainty of look-up tables, the angle uncertainty reduces at the same Mach number to  $u(y)=\pm 0.1^\circ$ .

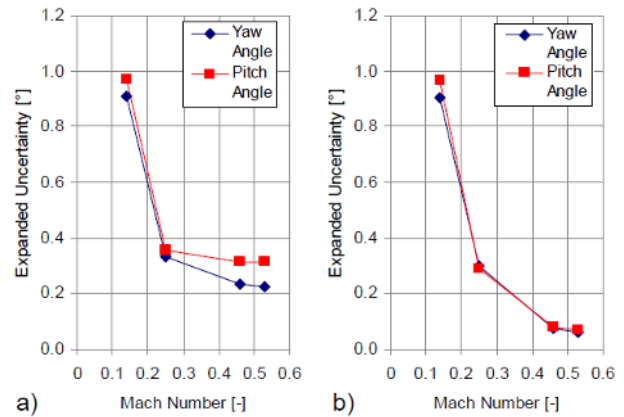


Fig. 9. Expanded uncertainty ( $k=2$ ) of the yaw and pitch angle derived with a) Calibration polynoms b) Look-up tables

## 5 Uncertainty of total and static pressure

### 5.1 Description of the measurement chain

The uncertainty evaluation for flow total and static pressure follows the same procedure as described in detail for the flow angles. For this reason, the following section will concentrate on specific issues related to the flow pressures.

The calibration of probe angle related total and static pressure is done in within the calibration procedure described in the previous section. The total pressure of the calibration region of the freejet is measured upstream in the nozzle. The difference to the flow region is determined analytically. The static pressure at the probe head can be derived from the atmospheric pressure.

#### 5.1.1 Step 1 – Model of the measurement chain

The calibration coefficients  $K_t$  and  $K_s$  are defined as follows:

$$K_t(\varphi, \gamma, Ma) = \frac{p_t - p_1}{q} \quad (15)$$

and

$$K_s(\varphi, \gamma, Ma) = \frac{p_t - p_s}{q} \quad (16)$$

with  $q$  as defined in equation (10).

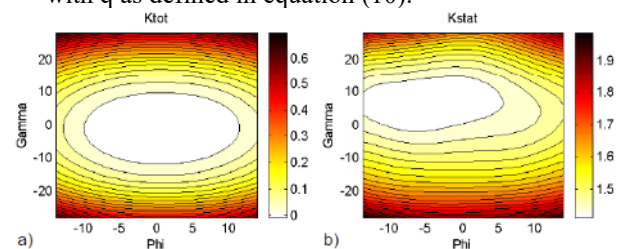


Fig. 10. Distribution of calibration coefficients with respect to yaw and pitch angles at  $Ma = 0.25$ , a)  $K_t$ , b)  $K_s$

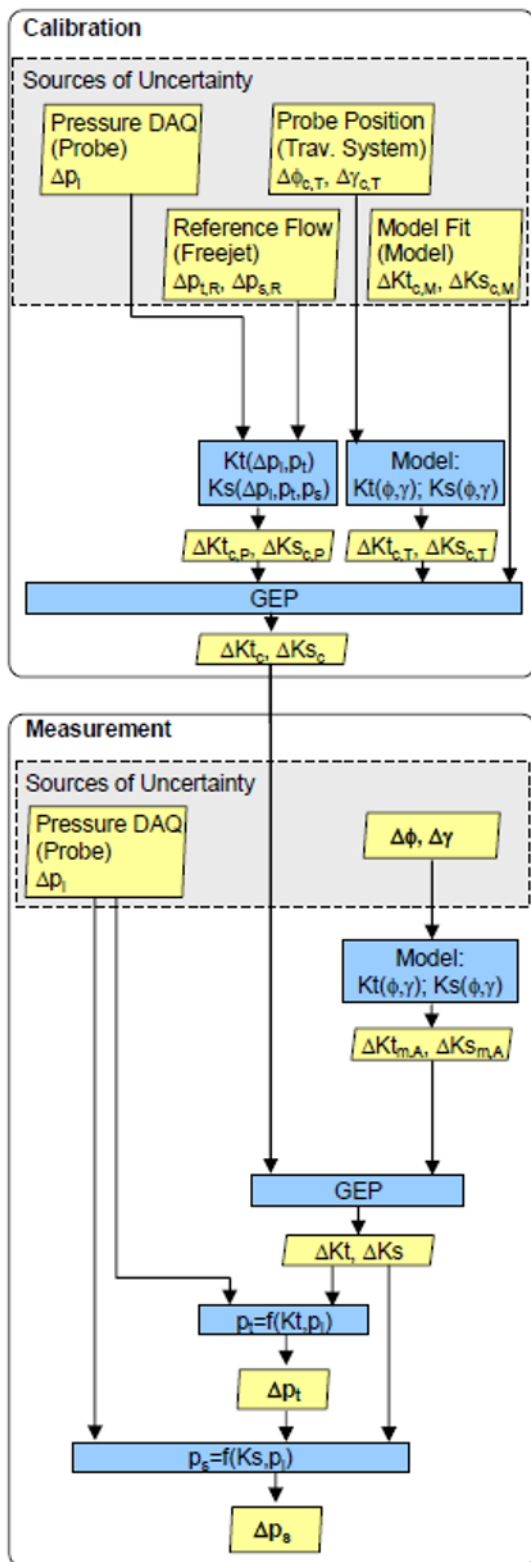


Fig. 11. Uncertainty propagation of total and static pressure measurement – Method A

Figure 10 shows the contours of  $K_t$  and  $K_s$  at a Mach number of  $Ma=0.25$ .  $K_t$  becomes zero at the probe center position since pressure at probe hole 1 is equal to the total pressure.

### 5.1.2 Step 2 – Uncertainty information

#### Probe Position, Reference Flow

The uncertainty introduced by the reference flow has already been described in the previous section. The accuracy of total and static depends on the differential pressure gauges of the freejet.

#### Model Fit

Similar to the angle post processing procedure the relation of calibration angles and calibration coefficients has to be change from

$$K_t(\phi, \gamma) \text{ and } K_s(\phi, \gamma) \quad (17)$$

to

$$\phi(K_t, K_s) \text{ and } \gamma(K_t, K_s) \quad (18)$$

For this operation the two options, polynomial approximation and look-up table are possible and have been evaluated.

#### Pressure DAQ

Uncertainties of the pressure data acquisition will propagate in this case into the calibration coefficients  $K_t$  and  $K_s$ . They have been analytically evaluated in the same way as described for the angle uncertainties.

#### Flow Angles

According to the procedure described in Figure 11 the flow angles are needed to determine the coefficients  $K_t$  and  $K_s$ . The procedure for determining these angles and their associated uncertainty has been explained in detail in the previous section.

### 5.1.3. Step 3 – Uncertainty calculation

According to the flow chart of Figure 11 the uncertainties have been calculated for a selection of calibrated angular positions each at 4 different Mach numbers.

### 5.1.4 Step 4 – Results

Figure 12 shows the shares of uncertainty of one example point at four different Mach numbers. In Figure 12 a) it can be seen that within the calibration the pressure measurement contributes the most to the uncertainty of the calibration coefficients  $K_t$  and  $K_s$ . In the presented case which uses calibration polynomials, the model fit uncertainty increases slightly with higher Mach numbers.

Figure 12 b) shows the uncertainty of the total pressure of calibration and measurement. In this graph the influence of the calibration is marked with the green bars. The measurements of the probe pressures and the atmospheric pressure have a Mach number independent constant contribution to the overall uncertainty. Everything that contributes

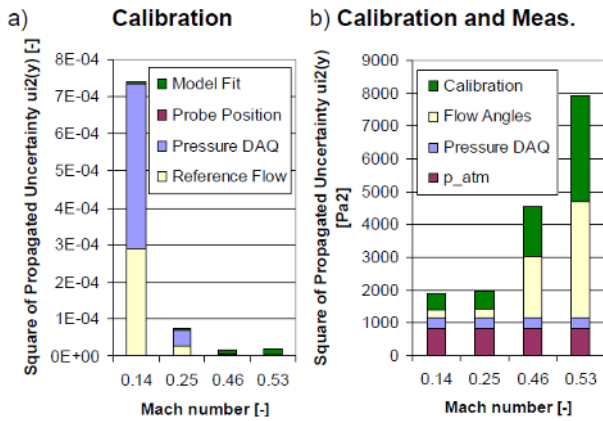


**Fig. 12.** Square of propagated uncertainties  $u_i^2(y)$  of 4 Mach numbers a) Calibration  $\Delta Kt^2$  [-] b) Calibration and measurement  $\Delta Pt^2$  [Pa<sup>2</sup>] (using Calibration polynoms)

to the uncertainty of the calibration coefficients  $Kt$  and  $Ks$  has an increased influence on the total overall uncertainty with increasing Mach numbers. This important effect is due to the following reason. The total pressure is calculated after equation (19).

$$p_t = p_1 + Kt \cdot \left( p_1 - \frac{1}{4} \sum_{i=2}^5 p_i \right) \quad (19)$$

The uncertainty of the first term, the absolute pressure  $P_1 = P_{atm} + dP_1$ , is rather unaffected by the Mach number.

The uncertainty of the second term, is defined by two counteracting, Mach number dependent effects. The calibration coefficient  $Kt$  decreases with increasing Mach number. However, its contribution to the overall uncertainty of  $Pt$  is influenced also by the partial derivative  $\partial Pt / \partial Kt$  which is the term  $q$  if equation (10). This term proportional to the dynamic head of the flow and is large at high Mach numbers. Therefore small uncertainties in  $Kt$  get amplified by  $q$  at high Mach numbers and result in higher uncertainties of the total pressure  $Pt$ .

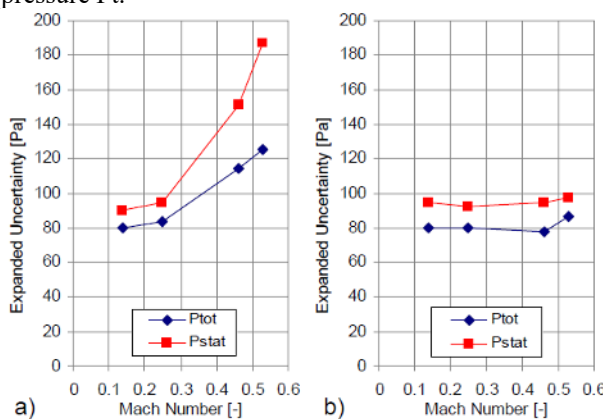


**Fig. 13.** Expanded uncertainty ( $k=2$ ) of the total pressure and static pressure derived with a) Calibration Polynoms b) Look-up tables

The same effect can be seen in Figure 13 a) which shows the averaged result of the extended uncertainty of 8 sample points that have been evaluated.

Figure 13 b) shows the overall pressure uncertainties if look-up tables are used. In this case the model fit uncertainty is assumed to be zero. Hence, the uncertainty

of the calibration and the flow angles reduces, which results in a nearly constant uncertainty of the flow pressures at the entire range of Mach numbers considered.

### 5.2 Alternative methods for deriving total and static pressure

The method for deriving total and static pressure presented in Figure 11 uses the flow yaw and pitch angle as input parameters for the calibration model. Since these angles are as well derived from a calibration model (see Figure 5) they will introduce an uncertainty to the total and static pressure. It is therefore reasonable to consider an alternative approach which uses directly the probe pressures as input values for a calibration model. Such an algorithm is presented in Figure 14. In this case the calibration coefficients  $Kt$  and  $Ks$  are directly related to  $K\phi$  and  $K\gamma$  in a calibration model. There are no angles needed to derive the pressure parameters.

$$Kt(K\phi, K\gamma) \text{ and } Ks(K\phi, K\gamma) \quad (20)$$

The disadvantage of this method is a higher uncertainty of the  $Kt$  and  $Ks$  coefficients, which gets propagated from the  $K\phi$  and  $K\gamma$  coefficients. In both, calibration and measurement these coefficients are calculated out of the probe pressures.

A comparison of both methods for determining total and static pressure comes to the following conclusion. If the uncertainty introduced by the fit of the calibration model can be neglected, both methods presented will be of similar uncertainty. The uncertainty of the calibration coefficients  $K\phi$  and  $K\gamma$  comes in through the flow angles in Method A (Figure 11), whereas in Method B (Figure 14) it goes into the calibration model of  $Kt$  and  $Ks$ . Only if the fit of the calibration models is less accurate, Method B would be advantageous, since only one calibration model has to be used to derive the pressures.

Another improvement can be made for the derivation of the static pressure by using a different definition for the coefficient  $Ks$

$$Ks(\phi, \gamma, Ma) = \frac{p_1 - p_s}{q} \quad (21)$$

In this case the uncertainty related to the total pressure can be removed (see equation (16)). This definition has been successfully used by Pfau [5].

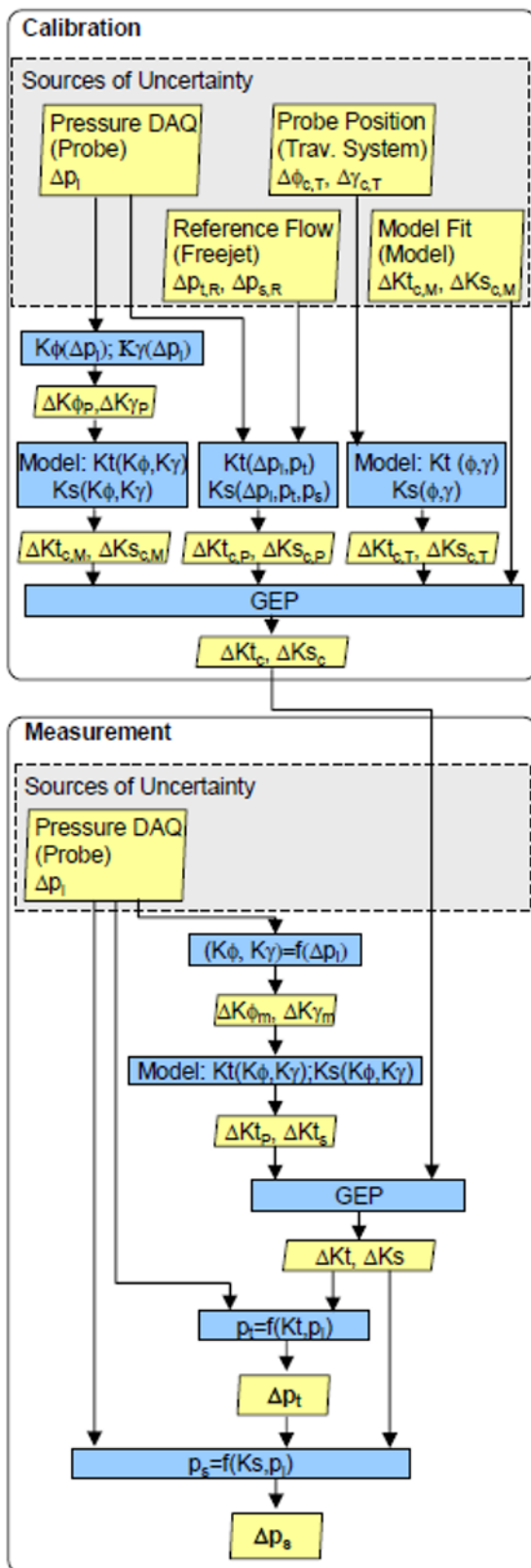


Fig. 14. Uncertainty propagation of total and static pressure measurement – Method B

## 6 Conclusions

The paper presents a probabilistic method for evaluating uncertainties in measurements and its application to pressure probe measurements in turbomachines. The

following conclusions can be drawn from the investigation:

Method

- The GUM [1] standard describes a conclusive, well structured and universal method for evaluating uncertainties in measurements.
- The method is able to combine different types of uncertainty information by converting all of them into probability distributions and propagating the uncertainties with the Gaussian error propagation formula.
- The resulting uncertainty statement contains the limits and the associated distribution of the measurement parameter. It is differentiated between standard and extended uncertainties (see Figure 15).

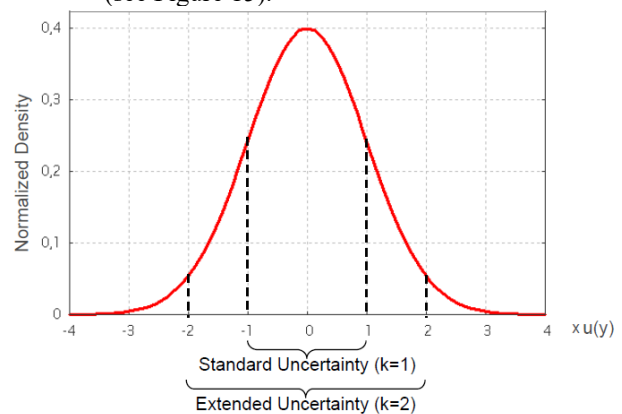


Fig. 15. Normalized normal distribution of uncertainty  $u(y)$  with marked range of standard and extended uncertainty

Uncertainty of Flow Angles

- The uncertainty of the probe pressure measurement has a significant influence on the flow angle uncertainty. It is advisable to keep the measured probe pressure within the favorable range of the pressure gauges, i.e. by having an adequate sensor back pressure or dedicated sensors for each pressure range.
- The fit of polynomial calibration models has a nearly constant contribution to the uncertainty over the Mach number range considered.
- It is suggested to use look-up tables instead of polynomial calibration models to reduce uncertainties due to polynomial data fitting.

Uncertainty of Flow Pressures

- The influence of the uncertainty of the calibration coefficients  $K_t$  and  $K_s$  on the total and static pressure uncertainties gets stronger with increasing Mach numbers. Therefore smaller uncertainties of the calibration coefficients at higher Mach numbers cause the overall uncertainty of the flow pressures to rise.
- Uncertainties of the calibration model can be reduced by the use of look-up tables.
- The use of models that relate the calibration coefficients  $K_t$  and  $K_s$  to  $K_\phi$  and  $K_\gamma$ , instead of  $\phi$  and  $\gamma$ , is found to cause similar uncertainty of the flow pressures, if the uncertainty due to the calibration model fit is low.

- The uncertainty of the static pressure can be reduced if the associated calibration coefficient does not include the flow total pressure.

## 7 Acknowledgments

The authors would like to thank D. Farenkopf, Dr. A. Pfau and Dr. R. Kessel for their support and helpful discussions during the preparation of this paper.

## References

1. ISO: *Guide to the Expression of Uncertainty in Measurement (GUM)*, 1st edition, 1993, corrected and reprinted 1995, International Organisation for Standardisation (Geneva, Switzerland), ISBN 92-67-1011889.
2. K. Weise, W. Wöger, *Messunsicherheit und Messdatenauswertung*, WILEY-VCH Verlag, ISBN 3-527-29610-7, 1999.
3. GUM Workbench®, Metrodata GmbH, [www.metrodata.de](http://www.metrodata.de).
4. T. Behr, A. I. Kalfas, R. S. Abhari, *Unsteady Flow Physics and Performance of a One-and-1/2-Stage Unshrouded High Work Turbine*, Proceedings of the ASME Turbo Expo 2006, GT2006-90959 (2006)
5. A. Pfau, *Loss Mechanisms in Labyrinth Seals of Shrouded Axial Turbines*, ETH dissertation No. 15226, ETH Zurich (2003)